

RESEARCH ARTICLE | AUGUST 01 2012

A miniature ultrabright source of temporally long, narrowband biphotons

Chih-Sung Chuu; G. Y. Yin; S. E. Harris



Appl. Phys. Lett. 101, 051108 (2012)

<https://doi.org/10.1063/1.4740270>



Export
Citation

CrossMark

Articles You May Be Interested In

Bright narrowband biphoton generation from a hot rubidium atomic vapor cell

Appl. Phys. Lett. (April 2017)

Temporally ultralong biphotons with a linewidth of 50 kHz

APL Photonics (December 2022)

Si–N linkage in ultrabright, ultrasmall Si nanoparticles

Appl. Phys. Lett. (June 2001)



Time to get excited.

Lock-in Amplifiers – from DC to 8.5 GHz



Find out more



Zurich
Instruments

A miniature ultrabright source of temporally long, narrowband biphotons

Chih-Sung Chuu,^{1,2,a)} G. Y. Yin,¹ and S. E. Harris¹¹Edward L. Ginzton Laboratory, Stanford University, Stanford, California 94305, USA²Department of Physics, National Tsing Hua University, Hsinchu 30013, Taiwan

(Received 19 April 2012; accepted 17 July 2012; published online 1 August 2012)

We demonstrate a miniature source of long biphotons utilizing the cluster effect and double-pass pumping in a monolithic doubly resonant parametric down-converter. We obtain a biphoton correlation time of 17.1 ns with a generation rate of 1.10×10^5 biphotons/(s mW) and an estimated linewidth of 8.3 MHz. © 2012 American Institute of Physics. [<http://dx.doi.org/10.1063/1.4740270>]

Ultrabright sources of temporally long and spectrally narrow photons are necessary for the realization of quantum networks where efficient interaction of light and matter at the single-photon level is essential.¹ Today, generation of such photons can be realized by using cold atoms and the techniques of cavity quantum electrodynamics^{2–5} and electromagnetically induced transparency.^{6,7} They may also be generated by using cavity-enhanced parametric down conversion followed by locked passive filtering.^{8–11} However the complexity of previous sources make them difficult, if not impossible, to scale up for quantum networks that have many nodes and require many generators.¹² In this letter we report an ultrabright source of long biphotons that uses a monolithic doubly resonant parametric down-converter without external filtering. At 700 μ W of pump power we obtain a biphoton correlation time of 17.1 ns with a generation rate of 1.10×10^5 photons/(s mW), a generated spectral brightness of 1.34×10^4 photons/(s MHz mW), and a count rate at the detector of 527 biphotons/(s mW).

Spontaneous parametric down conversion (SPDC) as usually practiced makes use of a forward-wave interaction where a pump photon splits into co-propagating signal and idler photons. The bandwidth of the biphotons is determined by the phase matching condition and thus the gain linewidth of the parametric interaction. For non-degenerate photons, it is $\Delta\omega_G = 1.77\pi/(|v_s^{-1} - v_i^{-1}|L)$, where v_s and v_i are the group velocities of the signal and idler photons and L is the length of the nonlinear crystal. For a KTP crystal with a length of 10 mm and type-II phase matching, the gain linewidth is about 4.66 cm^{-1} or 140 GHz. Because the linewidth of a strong radiative transition in an alkali metal is about 10 MHz, the bandwidth of these photons is about 10^4 times larger than that required for efficient interaction.

To reduce the photon bandwidth and increase the spectral brightness, one can resonate the signal and idler fields of the SPDC process with an external optical cavity^{13–15} to generate multi-longitudinal mode biphotons. One may then obtain a single-mode output by using additional spectral filtering.^{8,10,11} Using this technique with periodically poled KTP, Benson and colleagues⁸ have attained a count rate of 1000 biphotons/(s mW).

SPDC using a backward-wave interaction has also been suggested as a method to generate bright and temporally long biphotons.¹⁶ Its special feature is its narrow gain line-

width equal to $1.77\pi/(|v_s^{-1} + v_i^{-1}|L) \approx 0.026 \Delta\omega_G$. But realization of a backward-wave biphoton generator requires a KTP crystal that is periodically poled with a sub-micron periodicity; even with current structuring techniques¹⁷ this remains quite challenging.

In the present work, we demonstrate a monolithic doubly resonant parametric down-converter without external filtering. A schematic is shown in Fig. 1. We use a 10-mm long PPKTP crystal with spherically polished end faces (radii of curvature of about 10 mm). Both end faces are deposited with a high reflection coating at the signal and idler wavelengths so as to form a monolithic cavity at both frequencies. The finesse of the cavity is approximately 660. The pump is a single-frequency cw laser at 532 nm (linewidth < 5 MHz and power stability of $\pm 1\%$) and is tightly focused into the crystal. To implement double-pass pumping, one end face of the crystal is also deposited with a high reflection coating at the pump wavelength. Operating at 28 °C, with a temperature stability of better than 0.5 mK, and a few mW of pump, we generate collinear, orthogonally polarized signal and idler photons near degeneracy. This approach and the calculations that follow are motivated by both the backward wave calculations¹⁶ and earlier work that uses a monolithic design to obtain parametric oscillation in a single longitudinal mode.¹⁸

In order to obtain single mode operation without the need for filtering, the spacing of signal modes which are simultaneously resonant at the idler must be larger than the gain linewidth. Fig. 2 shows a comb of signal modes and a comb of idler modes where the mode spacing at the idler

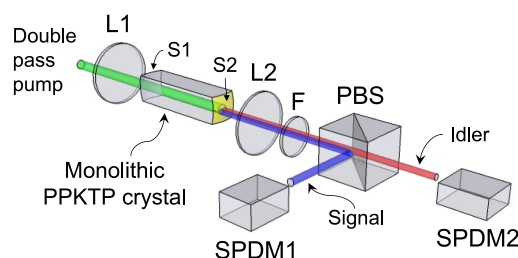


FIG. 1. Experimental setup. The biphoton source is composed of a periodically poled KTP crystal with spherically polished and coated end faces S1 and S2. So that the pump is double passed, the end face S2 is also coated at the 532 nm pump wavelength. Orthogonally polarized signal and idler photons are separated by a polarizing beam splitter (PBS) before detection by single-photon detection modules, SPDM1 and SPDM2. Long-pass and band-pass filters (F) are used to remove the pump and spurious fluorescence. Lens L1 and L2 are used to focus the pump into the crystal and to collimate the signal and idler beams.

^{a)}Electronic mail: cschuu@phys.nthu.edu.tw.

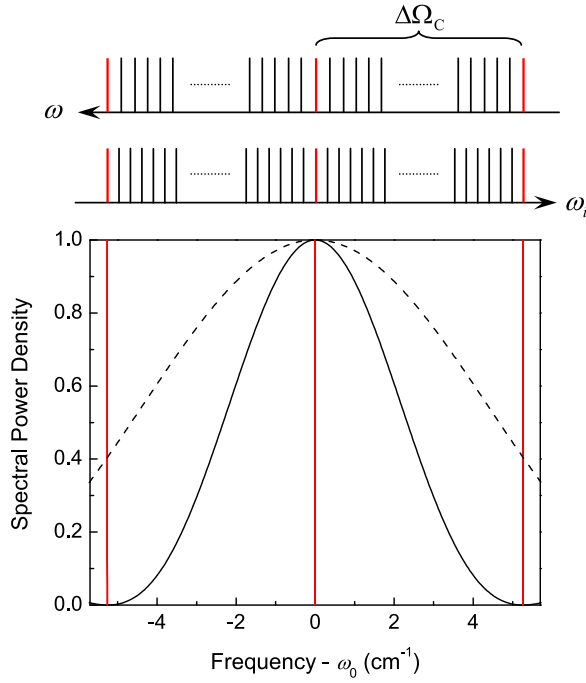


FIG. 2. Cluster spacing and gain linewidth. The top panel illustrates the signal and idler modes (shown in black color) increasing in opposite directions. The signal and idler resonances that line up vertically (red) are resonant at both the signal and the idler wavelengths. The bottom panel shows the calculated gain curve for SPDC with a double-pass pump (solid curve) and with a single-pass pump (dashed curve). The central cluster frequency (red vertical line) is taken as the center frequency of the gain curve ω_0 . Single-mode output is achieved when there is only one doubly resonant mode under the gain curve.

frequency Δ_i is slightly less than the mode spacing at the signal frequency Δ_s . Every so often, i.e., the red modes, a signal mode and an idler mode line up and are doubly resonant. Following the earlier literature,¹⁹ we term the frequency spacing of these doubly resonant modes as the cluster spacing $\Delta\Omega_C$. With the approximation that the mode spacing at the signal Δ_s and the idler frequency Δ_i are independent of frequency (no group velocity dispersion), the mode spacings of the signal and idler modes are related to their group velocities $v_{s,i}$ and the cavity length l by $\Delta_{s,i} = (2\pi)v_{s,i}/(2l)$. The cluster spacing is obtained by noting that since the difference of the mode spacings at the signal and idler is $(\Delta_s - \Delta_i)$, then a doubly resonant mode will occur after N idler modes, where $N \cong \Delta_s/(\Delta_s - \Delta_i)$. The cluster spacing at the signal frequency is then $N\Delta_i$ or

$$\Delta\Omega_C \cong \frac{\Delta_s \Delta_i}{\Delta_s - \Delta_i}. \quad (1)$$

We use Type II phase matching to increase the difference between the group velocities at the signal and idler wavelengths to thereby narrow the gain linewidth. To further narrow this linewidth, by what turns out to be an essential factor of two, the pump is double passed (Fig. 2) to effectively double the length of parametric interaction. To make the common cavity length as short as possible and to thereby increase the cluster spacing, we use a monolithic cavity. These ingredients, i.e., a monolithic cavity, type II phase matching, and double pass pumping work together to allow generation of single mode biphotons at both degenerate and

non-degenerate frequencies. In our experiment, the biphoton source is operated near degeneracy for maximum detector efficiency. The full width half power gain linewidth is 4.66 cm^{-1} and the cluster spacing is 5.26 cm^{-1} .

Following the methodology of Chuu and Harris,¹⁶ with $a_s^\dagger(\omega)$ and $a_s(\omega)$ denoting the signal frequency-domain operators, the spectral power density at the signal frequency is

$$S(\omega) = \int_{-\infty}^{\infty} \langle a_s^\dagger(\omega) a_s(\omega') \rangle \exp[i(\omega - \omega')t] d\omega' \\ = \frac{8\gamma_s \gamma_i \kappa^2}{\pi[4(\omega - \Omega_q)^2 + \Gamma_s^2][4(\omega - \Omega_q)^2 + \Gamma_i^2]} \quad (2)$$

and the bandwidth of the generated biphotons is $\Delta\omega = [(\sqrt{\Gamma_s^4 + 6\Gamma_s^2\Gamma_i^2 + \Gamma_i^4} - \Gamma_s^2 - \Gamma_i^2)/2]^{1/2}$. With r denoting the mirror reflectivity and $\xi_{s,i}$ as the single-pass power loss of the crystal, the output coupling rates are $\gamma_{s,i} = \Delta_{s,i}(1 - r)$ and the total cavity decay rates are $\Gamma_{s,i} = 2\xi_{s,i}\Delta_{s,i} + \gamma_{s,i}$. κ is the parametric coupling constant and $\Omega_q = q\pi v_s/l$ is the cold cavity frequency, where q is an integer.

With $a_s^\dagger(t)$ and $a_s(t)$ as the signal time-domain operators, the biphoton generation rate is given by $\langle a_s^\dagger(t) a_s(t) \rangle$ or

$$R = \int_{-\infty}^{\infty} S(\omega') d\omega' = \frac{4\gamma_s \gamma_i \kappa^2}{\Gamma_s \Gamma_i (\Gamma_s + \Gamma_i)} \quad (3)$$

at perfect phase matching. With $a_i^\dagger(t)$ and $a_i(t)$ as the idler time-domain operators, and τ equal to the difference in the arrival times of the signal and idler photons, the Glauber correlation function is

$$G^{(2)}(\tau) = \langle a_i^\dagger(t + \tau) a_s^\dagger(t) a_s(t) a_i(t + \tau) \rangle \\ = R^2 + \frac{4\kappa^2 \Gamma_s \Gamma_i}{(\Gamma_s + \Gamma_i)^2} \cdot \begin{cases} e^{\Gamma_s \tau} & , \tau < 0 \\ e^{-\Gamma_i \tau} & , \tau > 0 \end{cases} \quad (4)$$

The correlation function is thus characterized by two decay constants, one for $\tau < 0$, and the other for $\tau > 0$. Each decay constant is determined by the photon that arrives at the detector later in time (i.e., signal photons for $\tau < 0$ and idler photons for $\tau > 0$). For generation rates that are small as compared to these decay times, the Glauber correlation function can also be expressed in terms of the absolute square of the biphoton wave function as $G^{(2)}(\tau) = |\Psi(t, t + \tau)|^2$. The temporal width of the biphotons is then approximately $T_c = (\ln 2)(1/\Gamma_s + 1/\Gamma_i)$.

Experimentally, we find the monolithic down-converter straightforward to align and use. We tune the cavity by adjusting the temperature of the crystal. The calculated change of the center cluster frequency is about 5 GHz per degree. To select the cluster frequency nearest to the center of the gain profile, we adjust the temperature to maximize the intensity of parametric oscillation at a pump power of 50 mW. The oscillation wavelengths of the signal and idler (1063.5 nm and 1064.9 nm) are then measured by a wavemeter (Burleigh). The selected cluster frequency may or may not be at the center of the gain profile. For biphoton measurements we decrease the pump power to a few mW and, using single photon detection modules (id Quantique id400), fine

tune the temperature to maximize the biphoton generation rate. On the scale of seconds, the average generation rate fluctuates by about 10% about a mean rate that is stable on a scale of several hours.

We measure the Glauber correlation function by coincidence detection of the signal and idler photons. These photons are first separated by a polarizing beamsplitter and guided to the single-photon detection modules through multimode fibers. A digital time converter (FAST ComTec P7887) measures the coincidence counts as a function of delay. The counts are binned into 125-bin histograms. Accidental coincidence counts, primarily from residual pump (after back-reflection) and spurious fluorescence, are reduced with long-pass and band-pass filters. For a bin width T_b , the coincidence rate $R_c(\tau)$ is related the Glauber correlation function by $G^{(2)}(\tau) = R_c(\tau)/T_b$.

A typical measurement of the correlation function is shown in Fig. 3, where we use a pump power of 700 μ W. By fitting the measured curve with two asymmetric exponential decays for $\tau < 0$ and $\tau > 0$, we find $1/\Gamma_s = 11.33 \pm 0.12$ ns and $1/\Gamma_i = 13.29 \pm 0.14$ ns (the probable reason for the different decay times is the different reflectivity for the orthogonal polarizations). The correlation time (full width at half maximum) is then $T_c = 17.07 \pm 0.13$ ns. Using Eq. (2), the bandwidth of the generated biphotons is $\Delta\omega \cong 2\pi \cdot 8.3$ MHz.

The biphoton generation rate is obtained by summing the coincidence rates over all time delays and correcting for the quantum efficiency of the detectors (15% and 30% for the signal and idler), filter transmittance (53% in total for each channel), fiber system transmittance (70% and 60% for the signal and idler), and mirror reflectivity (95% in total for each channel). For the measurement of Fig. 3, we obtain an observed coincidence rate of 527 biphotons/(s mW). Correcting for the total collection efficiency, the generation rate and the generated spectral brightness of our biphoton source are $R = 1.10 \times 10^5$ biphotons/(s mW) and $R/\Delta\omega = 1.34 \times 10^4$ biphotons/(s MHz mW).

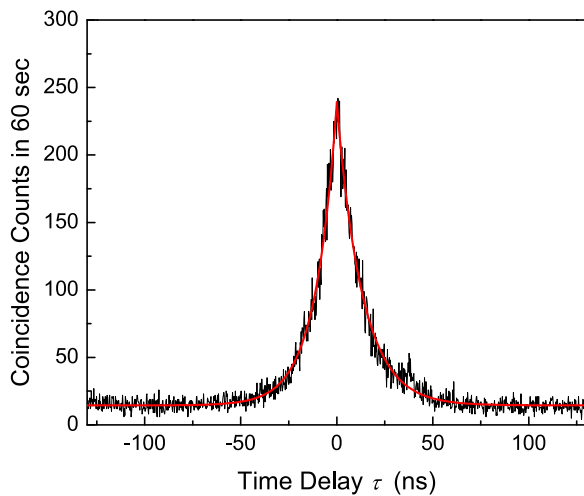


FIG. 3. Glauber correlation function of the signal and idler photons. The coincidence counts (black) are measured as a function of the time delay between the signal and idler photons at a pump power of 700 μ W. The red curve (theoretical) is a fit using two exponential decays with decay constants of $1/\Gamma_i = 13.29 \pm 0.14$ ns and $1/\Gamma_s = 11.33 \pm 0.12$ ns for τ greater than or less than zero. The full width at half maximum, or the correlation time, is $T_c = 17.07 \pm 0.13$ ns.

When the doubly resonant biphoton source is compared to a non-resonant SPDC of the same crystal length and pumping power, the generation rate is increased by a factor of η_r where

$$\eta_r \approx \frac{8\mathcal{F}}{\pi r^{1/2}} \frac{|v_s - v_i|}{(v_s + v_i)}, \quad (5)$$

and $\mathcal{F} \approx \pi r^{1/2}/(1-r)$ is the finesse of both cavities. The spectral brightness is increased by a factor of $\eta_b = \eta_r \Delta\omega_G/\Delta\omega$. For the present experiment the cavity has a finesse of $\mathcal{F} \approx 660$, and the enhancement, as compared to a non-resonant down-converter is $\eta_r \cong 40$ for the generation rate and $\eta_b \cong 16,000$ for the spectral brightness.

Time domain measurements, as described in the previous paragraph, are limited by the temporal resolution of the single photon detection modules of 250 ps. Because the spacing (in the frequency domain) of the cluster modes is 5.26 cm^{-1} and is much larger than the inverse of the temporal resolution, observation in the frequency domain is also desirable. Though the intensity of the biphoton source is too low to allow this observation, we have instead operated the generator in the oscillator regime and used a scanning Fabry Perot interferometer (FSR of 2 GHz and spectral resolution of 65 MHz) to determine that only a single mode is oscillating. Though promising, this does not rule out the possibility of biphoton generation in a distant cluster mode that is not discernible by time domain correlation.

To verify that the biphotons are generated in nearly a single transverse mode, we have replaced the multimode fibers used for the time domain measurements with single mode fibers and find that the ratio of the observed biphoton generation rate for the single mode case to that of the multimode case is 0.78.

The monolithic down-converter, as designed, generates time energy entangled photons, but not polarization entangled photons. To produce biphotons that are polarization entangled, while retaining type II phase matching, one may periodically pole the nonlinear crystal with two periodicities that simultaneously allow the parametric process where the signal is an ordinary wave and the idler is extraordinary and the process where the signal is extraordinary and the idler is ordinary.²⁰

One may envision the use of monolithic down-converters such as described here to allow the quantum repeater protocol¹² with one wavelength in the telecommunication band and one wavelength that accesses a storage medium.^{21–24} For example a 525 nm pumped source could readily be designed with wavelengths at 1.55 μ m and 0.8 μ m. The 1.55 μ m photons would travel through fibers to a distant beam splitter while the nominally 0.8 μ m photons would be incident on nearby atomic ensembles. Efficient storage and extraction both require narrow band photons as described here. This monolithic source might also be used for generating conditional long single photons that may be amplitude or phase modulated by high-speed light modulators.^{25–28}

In summary, this work has shown that an appropriately designed doubly resonant monolithic crystal may be used as a parametric down-converter to generate temporally long and spectrally narrow biphotons with exceedingly high

spectral brightness. Application to several areas of quantum information processing seems likely. To further increase the biphoton correlation time and the brightness, and reduce the bandwidth, all by a factor of about 2, one could use the monolithic cavity described in Ref. 18 which has a higher finesse of $\mathcal{F} = 1300$.

This work was supported by the U.S. Air Force Office of Scientific Research (FA9550-10-1-0055), the U.S. Army Research Office, and the Taiwan National Science Council (101-2112-M-007-001-MY3).

- ¹H. J. Kimble, *Nature (London)* **453**, 1023 (2008).
- ²A. Kuhn, M. Hennrich, and G. Rempe, *Phys. Rev. Lett.* **89**, 067901 (2002).
- ³H. P. Keller, B. Lange, K. Hayasaka, W. Lange, and H. Walther, *Nature (London)* **431**, 1075 (2004).
- ⁴J. McKeever, A. Boca, A. D. Boozer, R. Miller, J. R. Buck, A. Kuzmich, and H. J. Kimble, *Science* **303**, 1992 (2004).
- ⁵J. K. Thompson, J. Simon, H. Loh, and V. Vuletić, *Science* **313**, 74 (2006).
- ⁶V. Balić, D. A. Braje, P. Kolchin, G. Y. Yin, and S. E. Harris, *Phys. Rev. Lett.* **94**, 183601 (2005).
- ⁷S. Du, P. Kolchin, C. Belthangady, G. Y. Yin, and S. E. Harris, *Phys. Rev. Lett.* **100**, 183603 (2008).
- ⁸M. Scholz, L. Koch, R. Ullmann, and O. Benson, *Appl. Phys. Lett.* **94**, 201105 (2009).
- ⁹E. Pomarico, B. Sanguinetti, N. Gisin, R. Thew, H. Zbinden, G. Schreiber, A. Thomas, and W. Sohler, *New J. Phys.* **11**, 113042 (2009).
- ¹⁰F. Wolfgramm, Y. A. de Icaza Astiz, F. A. Beduini, A. Cerè, and M. W. Mitchell, *Phys. Rev. Lett.* **106**, 053602 (2011).
- ¹¹H. Zhang, X.-M. Jin, J. Yang, H.-N. Dai, S.-J. Yang, T.-M. Zhao, J. Rui, Y. He, X. Jiang, F. Yang *et al.*, *Nat. Photonics* **5**, 628 (2011).
- ¹²N. Sangouard, C. Simon, H. de Riedmatten, and N. Gisin, *Rev. Mod. Phys.* **83**, 33 (2011).
- ¹³Z. Y. Ou and Y. J. Lu, *Phys. Rev. Lett.* **83**, 2556 (1999).
- ¹⁴C. E. Kuklewicz, F. N. C. Wong, and J. H. Shapiro, *Phys. Rev. Lett.* **97**, 223601 (2006).
- ¹⁵M. Scholz, L. Koch, and O. Benson, *Phys. Rev. Lett.* **102**, 063603 (2009).
- ¹⁶C.-S. Chuu and S. E. Harris, *Phys. Rev. A* **83**, 061803(R) (2011).
- ¹⁷C. Canalias and V. Pasiskevicius, *Nat. Photonics* **1**, 459 (2007).
- ¹⁸T. Ikegami, S. Slyusarev, T. Kurosu, Y. Fukuyama, and S. Ohshima, *Appl. Phys. B* **66**, 719 (1998).
- ¹⁹R. C. Eckardt, C. D. Nabors, W. J. Kozlovsky, and R. L. Byer, *J. Opt. Soc. Am. B* **8**, 646 (1991).
- ²⁰K. Thyagarajan, J. Lugani, S. Ghosh, K. Sinha, A. Martin, D. B. Ostrowsky, O. Alibart, and S. Tanzilli, *Phys. Rev. A* **80**, 052321 (2009).
- ²¹T. Chanelière, D. Matsukevich, S. D. Jenkins, S.-Y. Lan, T. A. B. Kennedy, and A. Kuzmich, *Nature (London)* **438**, 833 (2005).
- ²²C.-S. Chuu, T. Strassel, B. Zhao, M. Koch, Y.-A. Chen, S. Chen, Z.-S. Yuan, J. Schmiedmayer, and J.-W. Pan, *Phys. Rev. Lett.* **101**, 120501 (2008).
- ²³B. Zhao, Y.-A. Chen, X.-H. Bao, T. Strassel, C.-S. Chuu, X.-M. Jin, J. Schmiedmayer, Z.-S. Yuan, S. Chen, and J.-W. Pan, *Nat. Phys.* **5**, 95 (2009).
- ²⁴R. Zhao, Y. O. Dudin, S. D. Jenkins, C. J. Campbell, D. N. Matsukevich, T. A. B. Kennedy, and A. Kuzmich, *Nat. Phys.* **5**, 100 (2009).
- ²⁵P. Kolchin, C. Belthangady, S. Du, G. Y. Yin, and S. E. Harris, *Phys. Rev. Lett.* **101**, 103601 (2008).
- ²⁶C. Belthangady, S. Du, C.-S. Chuu, G. Y. Yin, and S. E. Harris, *Phys. Rev. A* **80**, 031803(R) (2009).
- ²⁷H. P. Specht, J. Bochmann, M. Mücke, B. Weber, E. Figueroa, D. L. Moehring, and G. Rempe, *Nat. Photon.* **3**, 469 (2009).
- ²⁸C. Belthangady, C.-S. Chuu, I. A. Yu, G. Y. Yin, J. M. Kahn, and S. E. Harris, *Phys. Rev. Lett.* **104**, 223601 (2010).